Journal of Cellular Biochemistry 99:807–815 (2006)

2-(4-Methylphenyl)-1,3-Selenazol-4-One Induces Apoptosis by Different Mechanisms in SKOV3 and HL 60 Cells

Hak Jun Ahn,[1] Mamoru Koketsu,[2] Eun Mi Yang,[1] Yong Man Kim,[3] Hideharu Ishihara,[2] and Hyun Ok Yang[1]*

[1]Natural Products Research Division, Korea Institute of Science and Technology, Gangneung Institute, Daejeon-dong, Gangneung, Gangwon-do, 210-340, Republic of Korea
[2]Department of Chemistry, Faculty of Engineering, Gifu University, Gifu 501-1193, Japan
[3]Department of Obstetrics and Gynecology, College of Medicine, University of Ulsan, Asan Medical Center, Seoul, Korea

Abstract We examined the ability of the synthetic selenium compound, 2-(4-methylphenyl)-1,3-selenazol-4-one (hereafter designated **3a)**, to induce apoptosis in a human ovarian cancer cell line (SKOV3) and a human leukemia cell line (HL-60). Flow cytometry showed that **3a** treatment induced apoptosis in both cell lines to degrees comparable to that of the positive control, paclitaxel. Apoptosis was measured by PS externalization, DNA fragmentation and decreased mitochondrial membrane potential (MMP). However, analysis of the mechanism of action revealed differences between the responses of the two cell lines. Treatment with **3a** arrested the cell cycle and induced caspase-3 activation in HL-60 cells, but not in SKOV3 cells. In contrast, **3a** treatment induced apoptosis through translocation of AIF, a novel pro-apoptotic protein, in SKOV3 cells, but not in HL-60 cells. Collectively, our data demonstrated that **3a** induced apoptosis in both cell lines, but via different action mechanisms. J. Cell. Biochem. 99: 807–815, 2006.

Key words: selenium; apoptosis; AIF; caspase; mitochondria

First discovered in 1817, the element selenium is found as a red amorphous powder, a glass-like substance, or a gray metal. The uses and properties of selenium have proven controversial over time. It was considered a dangerous poison until it was identified as a growth factor for certain bacteria and an essential trace element for rats. Similarly, selenium was once thought to be carcinogenic, but it is now under consideration as an agent for cancer prevention. And finally, selenium is sold in supermarkets as an antioxidant, yet toxicologists have noted that selenium is able to undergo pro-oxidant redox cycling [Flohe et al., 2000]. A landmark study by Clark et al. [1991] showed that a Se supplement had cancer chemopreventive effects in humans. More recent studies have confirmed the cancer chemopreventive activity of selenium [Ganther, 1999] and have suggested that this effect may be related to selenium-induced apoptosis of cancer cells. Indeed, several groups have shown that selenocompounds, as Se-methylselenocystein, induce apoptosis in cell culture systems [Lu et al., 1994; Cho et al., 1999; Shen et al., 1999]. Other studies revealed that selenium exhibited inhibitory effects in various tumor cell lines and acted against chemically induced and transplanted tumors [Ip, 1985]. However, the mechanism by which selenium inhibits tumorigenesis in vivo and cell growth in vitro remains to be eludicated.

Lu et al. [1995] showed that selenite inhibits the growth of mammary cancer cells specifically

Grant sponsor: Plant Diversity Research Center of 21st Century Frontier Research Program, Ministry of Science & Technology, Republic of Korea; Grant number: PF0320503-00; Grant sponsor: KIST institutional program; Grant number: 2Z 02900.

*Correspondence to: Dr. Hyun Ok Yang, Natural Products Research Division, Korea Institute of Science and Technology-Gangneung Institute, Deajeon-dong, Gangneung, Gangwon-do, 210-340, Republic of Korea.
E-mail: hoyang@kist.re.kr

Received 1 December 2005; Accepted 26 March 2006
DOI 10.1002/jcb.20973

in the late S and early G2 phases of the cell cycle. In addition, the authors reported that selenite induces single strand DNA breaks more rapidly than organic selenium compounds, and hypothesized that selenite has non-specific effects on cell growth in vitro in contrast to the more specific effects of organic compounds. Clinical studies revealed that Se reduced the side effects of cancer chemotherapeutic agents and improved the immune status of treated cancer patients, indicating that Se holds promise in both cancer prevention and tumor therapy [Schrauzer, 2000].

We recently reported the generation of 1,3-selenazol-4-one (here after called **3a)**, by reaction of primary selenoamides with α-haloacyl halides in the presence of pyridine [Koketsu et al., 2001]. In the present study, we investigated the mechanisms underlying apoptosis induced by treatment with **3a** in SKOV3 and HL-60 cells, as compared to that induced by the positive control, taxol. [Ahn et al., 2004]

MATERIALS AND METHODS

Synthesis of 2-(4-Methylphenyl)-1,3-Selenazol-4-One

3a was prepared according to the previously reported procedure [Koketsu et al., 2001]. Briefly, chloroacetyl chloride (0.12 g, 1.0 mM) in dry dichloromethane (5 ml) was added dropwise (with stirring) to a solution of 4-methyl benzeneselenoamide (0.20 g, 1.0 mM) in dry dichloromethane (5 ml) at 0°C under an argon atmosphere. The reaction mixture was stirred for 1 h at room temperature, and then dry pyridine (0.16 g, 2.0 nM) in dry dichloromethane (5 ml) was added dropwise at 0°C. The reaction mixture was stirred for 2 h at 0°C, extracted with dichloromethane (100 ml), and then washed with water (30 ml). The organic layer was dried over sodium sulfate and evaporated to dryness. The residue was purified by flash chromatography on silica gel with dichloromethane to yield **3a** (0.19 g, yield: 80%).

Cell Culture

The human ovarian SKOV3 carcinoma cell line was obtained from the American Tissue Culture Collection (ATCC, HTB-77) and grown at 37°C in RPMI 1640 supplemented with 10% fetal bovine serum, 1% L-glutamine, and 1% penicillin/streptomycin (pH 7.4) in a humidified atmosphere containing 5% CO_2. The human leukemia cell line, HL-60 was obtained from the ATCC, (CCL 240) and grown at 37°C in Iscove's Modified Dulbecco's Medium (IMDM) supplemented with 20% fetal bovine serum, 25 mM HEPES, 1% L-glutamine, and 1% penicillin/streptomycin (pH 7.4) in a humidified atmosphere containing 5% CO_2. All cell culture reagents were purchased from Gibco BRL (Grand Island, NY).

Cytotoxicity

The cytotoxicity of **3a** and taxol (positive control) was evaluated by measuring lactate dehydrogenase (LDH) activity in the media 24 h after drug exposure. Briefly, SKOV3 and HL-60 cells were seeded at 2×10^4 cells per well or 1×10^5 cells per well, respectively, and incubated with the indicated doses of taxol or **3a** for 24 h at 37°C in a humidified atmosphere containing 5% CO_2. Cells were then subjected to the CytoTox96 non-radioactive assay according to manufacture's protocol (Promega, WI), followed by spectrophotometric analysis at 490 nm.

Determination of Cell Cycle and DNA Fragmentation

For analysis of DNA fragmentation and cell cycle, cells were harvested, resuspended to 1×10^6 cells/ml, washed with PBS, and fixed in ice-cold 70% ethanol for 1 h at 4°C. After centrifugation, cells were resuspended, incubated for 30 min in PBS containing 0.5 mg/ml RNase A and 40 μg/ml PI at 37°C, and analyzed with a FACSCalibur flow cytometer (Becton Dickson, San Jose, CA) as previously described [Ormerod et al., 1992].

Measurement of Phosphatidylserine (PS) Externalization and Chromatin Condensation

PS externalization was examined with a two-color analysis of FITC-labeled annexin V binding and PI uptake using flow cytometry and a Leica TCS SP2 confocal microscope (Leica, Germany). Briefly, cells were stained according to the manufacturer's instructions. Flow cytometry was performed on a FACSCalibur flow cytometer (Becton Dickson), and data acquisition and analysis were performed using the CellQuest software package (Becton Dickson). Annexin V/PI dot plots were sectioned and analyzed as previously reported [Van Engeland et al., 1996; Ahn et al., 2004], for identification of living cells (annexin V^-/PI^-), early apoptotic cells (annexin V^+/PI^-), late apoptotic cells

(annexin V^+/PI^+), and necrotic cells (annexin V^-/PI^+).

Detection of Mitochondrial Membrane Potential ($\Delta\psi m$)

The mitochondrial membrane potential (MMP) was analyzed using JC-1, a lipophilic cationic fluorescence dye that selectively enters mitochondria and acts as a dual emission probe by reversibly changing color from red-orange color (FL-2) to green (FL-1) as the mitochondrial membrane becomes more depolarized [Cossarizza et al., 1993]. SKOV3 and HL-60 cells were seeded at 1×10^6 and 5×10^3 cells per well and incubated with 5 μg/ml JC-1 (prepared as a 5 mg/ml stock in DMSO) for 30 min at 37°C in the dark. Cells were then washed with PBS at 4°C, and analyzed by FACSCalibur flow cytometry and Leica TCS SP2 confocal microscopy.

Caspase Activation Assay

Activated caspase-3 was analyzed with the Carboxyfluoresence in FLICA Apoptosis Detection Kit (Serotec, UK), according to the manufacturer's protocol. This novel methodology is based on a Fluorochrome Inhibitor of Caspases (FLICA). Experiments using green fluorescence, such as ours, use a carboxyfluorescein-labeled fluoromethyl ketone peptide caspase inhibitor [Ekert et al., 1999]. The results were analyzed by FACSCalibur flow cytometry.

Western Blot Analysis

Cells were scraped, washed with ice-cold PBS, and then 2×10^6 cells per control or treatment group were lysed in 100 μl lysis buffer (50 mM Tris, 150 mM NaCl, 10% SDS, 1% NP-40, 1% Triton X-100 and 1 mM EGTA) containing protease inhibitors (1 mM PMSF, 1 μM Pepstatin, 1 μM Leupeptin, and 0.3 μM Aprotinin; Sigma). After 1 h incubation on ice, the lysates were centrifuged at 15,000*g* for 15 min at 4°C, and the protein content in each supernatant was determined using the Bio-Rad Protein Assay Dye Reagent (Bio-Rad). Each supernatants were mixed with sample buffer (60 mM Tris-HCl, pH 6.8, 2% SDS, 10% glycerol, 140 mM mercaptoethanol and 0.002% bromophenol blue), boiled for 5 min and resolved on an SDS–polyacrylamide gel (100 μg protein/lane). Proteins were electrotransferred onto PVDF membrane and immunoblotted with anti-pro-caspase-3 (1:1,000 dilution) or anti-bcl-2 (1:1,000 dilution) antibodies. Detection was performed with appropriate HRP-conjugated secondary antibodies (1:5,000 dilution) (Jackson ImmunoResearch, PA) and an enhanced chemiluminescence reagent (Pierce. Denmark).

Detecting the Translocation of Apoptosis Inducing Factor (AIF)

The translocation of AIF in SKOV3 and HL-60 cells was determined by confocal microscopy. Treated and control cells were grown on coverslips, washed with PBS, fixed with 4% paraformaldehyde in PBS at room temperature for 1 h, and permeabilized with 0.3% Triton X-100 at room temperature for 30 min before incubation with rabbit anti-AIF (Upstate, VA) (0.5 μg/ml) for 12 h at 4°C. After three washes in PBS, cells were incubated with biotin-conjugated secondary antibodies (2 μg/ml) for 4 h at 4°C, and then stained with Alexa Fluor 488 dye (1:500 dilution; (Molecular Probes, MO)) for 1 h at room temperature. Cells were washed three times with PBS and then mounted with DAKO fluorescent mounting medium (DAKO, Carpinteria, CA) and observed under Leica TCS SP2 confocal microscopy. And 5×10^6/ml, HL-60 cells, that was suspended cell line, was performed spin down for attach onto cover glass with cytospin at 700 rpm for 5 min and observed under Leica TCS SP2 confocal microscopy.

RESULTS

Cytotoxicity

We first sought to determine the cytotoxic effects of **3a** on SKOV3 and HL-60 cells under our culture conditions, as compared to that of the positive control, taxol. Cell death was evaluated by measuring LDH release into the media from dead or dying cells 24 h after drug treatment. LDH release is a reliable biochemical indicator of cell death in these cell lines, and could easily be used on large-scale experiments such as ours. Our results revealed that the IC_{50} of taxol was 2.3 ± 0.2 μM in SKOV3 cells and 3.2 ± 0.5 μM in HL-60 cells, while the IC_{50} values of **3a** were 31.53 ± 1.35 μM and 35.95 ± 6.8 μM, respectively.

DNA Fragmentation

To investigate the type of cell death induced by **3a** and taxol in SKOV3 and HL-60 cells, PS externalization and PI uptake were analyzed by flow cytometry. Figure 1a shows a dot plot of four quadrants scaled with logarithms, representing the fluorescence levels

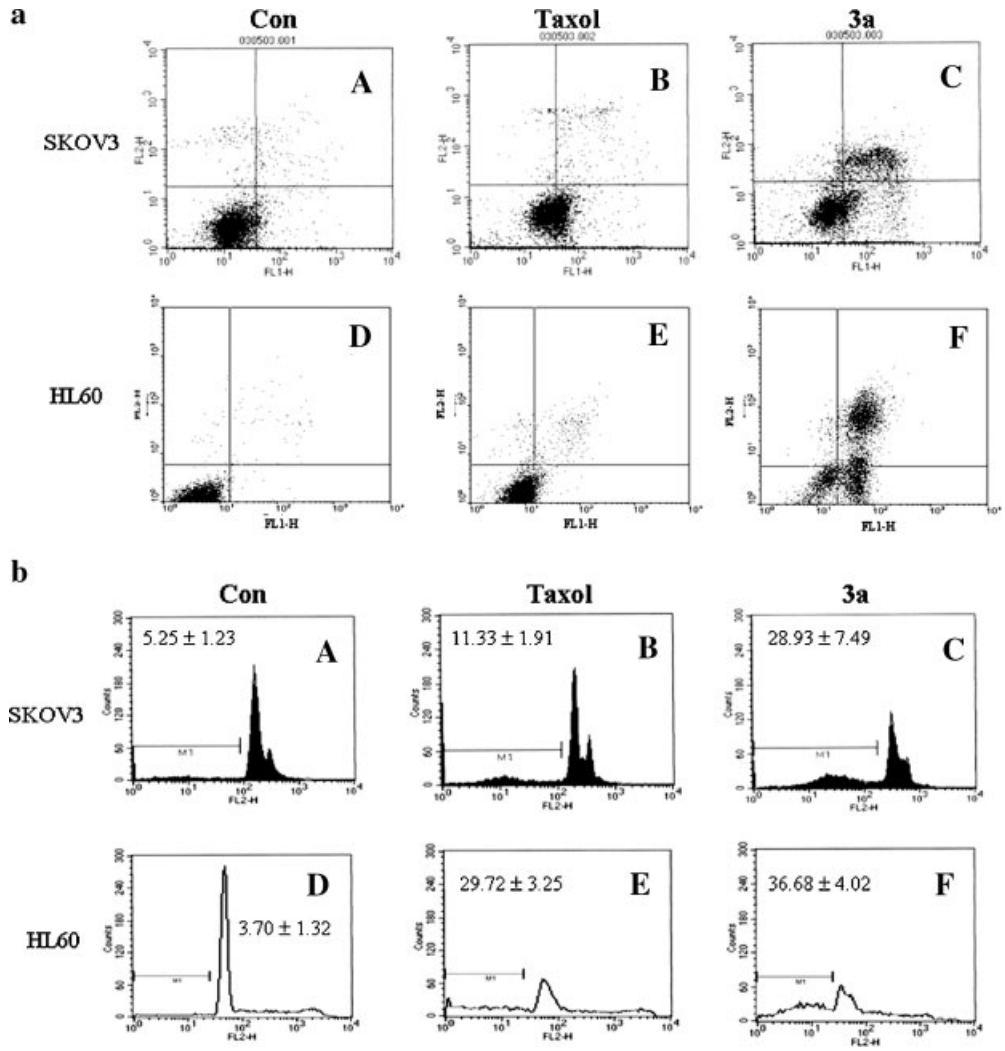

Fig. 1. Staining with annexin V/ PI and DNA fragmentation rate. **a**: **3a** and taxol induced early-and late-stage apoptosis in SKOV3 and HL-60 cells. **A** and **D**, untreated cells; **B** and **E**, cells treated with 5 μM of taxol; **C** and **F**, cells treated with 45 μM of **3a**. Each sample was measured 24 h post-treatment. Cells undergoing early apoptosis stained positive for only Annexin V (conjugated FITC), it was shown lower right panel, while those that had progressed to late apoptosis stained positive for both Annexin V and Propidium iodide (PI), it was shown upper right panel due to disruption of the plasma membrane. **b**: **A** and **D**, untreated cells; **B** and **E**, cells treated with 5 μM of taxol; **C** and **F**, cells treated with 45 μM of **3a**. Sub-G1 phase populations were increased by twofold (11.33 ± 1.91, B) and sixfold (28.93 ± 7.49, C) in SKOV3 cells compared to controls (5.25 ± 1.23), and by eightfold (29.72 ± 3.25, E) and tenfold (36.68 ± 4.02, F)† in HL-60 cells compared to controls (3.70 ± 1.32)†. †, (mean ± SD, $P < 0.05$). The M1 bar under the G1 phase cells represents the mean DNA fragmentation because Maximun peak was mean the G1 phase.

of FITC-labeled annexin V (FL-1H) and PI (FL-2H), respectively. Our results revealed that treatment with 45 μM **3a** increased the number of cells in the early stage of apoptosis (annexin V^+/PI) by fivefold in SKOV3 cells, and that treatment with 5 μM taxol showed similar effects. In contrast, HL-60 cells showed a ~30-fold increase in early apoptotic cells in response to 45 μM **3a**, but only a fourfold increase in response to 5 μM taxol.

PI staining was used to examine the nuclear events after **3a** treatment. Chromatin condensation was seen in **3a**-treated cells. In addition, **3a**-treated SKOV3 cells showed up to sixfold increases in the sub-G1 population ($P < 0.05$) when compared with control cells. In HL-60 cells, **3a** treatment induced a 10-fold increase in the sub-G1 population (Fig. 1b).

3a Induces Caspase-3 Activation in HL 60 But not SKOV3 Cells

The caspases are key factors in the apoptotic pathway [Zamzami and Kroemer, 1999], with caspase-3 playing a critical role in apoptosis.

Here, we examined whether **3a** treatment induced apoptosis in a caspase-3-dependent manner in SKOV3 and/or HL-60 cells. Western blot analysis suggested that treatment with **3a** (45 μM) or taxol (5 μM) resulted in caspase-3 activation only in HL-60 but not SKOV3 cells (Fig. 2). However, activation of caspase-3 in HL-60 cells increased threefold (4.24 ± 0.34) following **3a** treatment, and twofold (3.21 ± 0.75) following taxol treatment, as compared with untreated controls (1.43 ± 0.27) with FLICA assay by flow cytometry. These results suggest that the mechanism of apoptotic induction may differ between the two cell lines.

3a Induces Mitochondrial Depolarization

Mitochondrial membrane depolarization is an early event of apoptosis that increases mitochondrial membrane permeability (MMP) and facilitates the release of pro-apoptotic factors such as cytochrome-*c* and AIF into the cytosol [Cande et al., 2002; Ravagnan et al., 2002]. To assess mitochondrial depolarization in **3a-** and taxol-treated cells, we used JC-1, a mitochondria-specific, lipophilic cationic fluorescence dye. The green-fluorescent JC-1 probe (emission maxima ~530 nm) exists as a monomer at low concentration or at low MMP. However, at higher concentration or higher potential, JC-1 forms red-fluorescent J-aggregates that exhibit a broad excitation spectrum and an emission maximum at ~590 nm. As shown in Figure 3a, the fluorescence intensity at 530 nm increased significantly in **3a**- and taxol-treated SKOV3 cells as compared to untreated controls (6.56 ± 0.03 and 4.51 ± 0.83, respectively, vs. 2.77 ± 0.90; $P < 0.05$ in both cases) (Fig. 3b,c) and untreated HL60 cells showed mostly greenish orange mitochondria, too. It was mean untreated HL60 cells (3.71 ± 0.22) maintained their MMPs highly, while taxol- and **3a**-treated HL60 cells showed increased green fluorescence in 11.84 ± 3.71 and 16.01 ± 0.36 of cells, respectively, indicating that the MMP were decreased like SKOV3 cells (Fig. 3b,c). We tried to analyze these fluorescence data using flow cytometry.

AIF Translocates Into the Nucleus in Response to 3a Treatment in SKOV3 But not HL-60 Cells

The AIF protein is a caspase-independent pro-apoptotic factor released from mitochondria and translocated into nucleus [Susin et al., 1999]. However, the precise connection between AIF and MMP is not completely clear in caspase-independent apoptosis. Here, we used confocal microscopy to examine AIF translocation in response to **3a** treatment of SKOV3 and HL-60 cells stained with an FITC-conjugated anti-AIF antibody (green fluorescence). Confocal microscopy revealed that AIF was present in the cytosol of untreated cells, presumably in the mitochondria. SKOV3 cells treated with **3a** or taxol showed nuclear localization of AIF, indicating the AIF translocation known to be a hallmark of caspase-independent apoptosis (Fig. 4). In contrast, we observed no evidence of AIF translocation in HL-60 cells treated with **3a** or taxol. These data suggest that mitochondria may play a role in triggering both caspase-independent and -dependent apoptotic pathways.

DISCUSSION

While selenium biochemistry has gained recent attention, many aspects of its effects on natural systems remain unexplored [Flohe et al., 2000]. Although several mechanisms have been proposed for these cancer chemopreventive

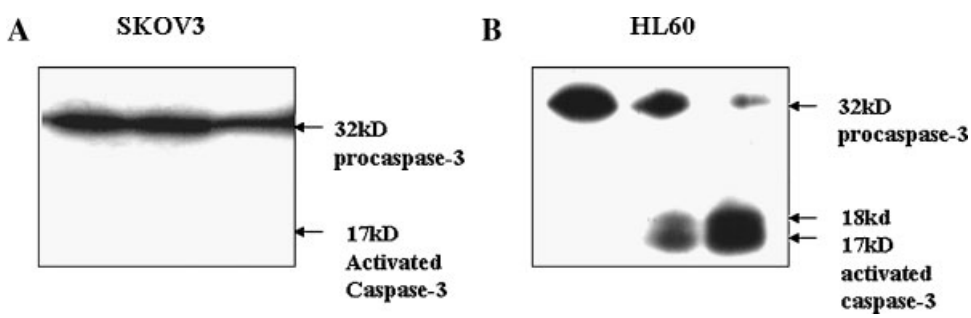

Fig. 2. Western blotting of caspase-3 activation. **A**: SKOV3 and **B**: HL-60 cells. **Lane 1**, untreated cells; **lane 2**, cells treated with 5 μM of taxol; **lane 3**, cells treated with 45 μM of **3a**. Treatment with **3a** or taxol induced caspase-3 activation in HL-60 but not SKOV3 cells.

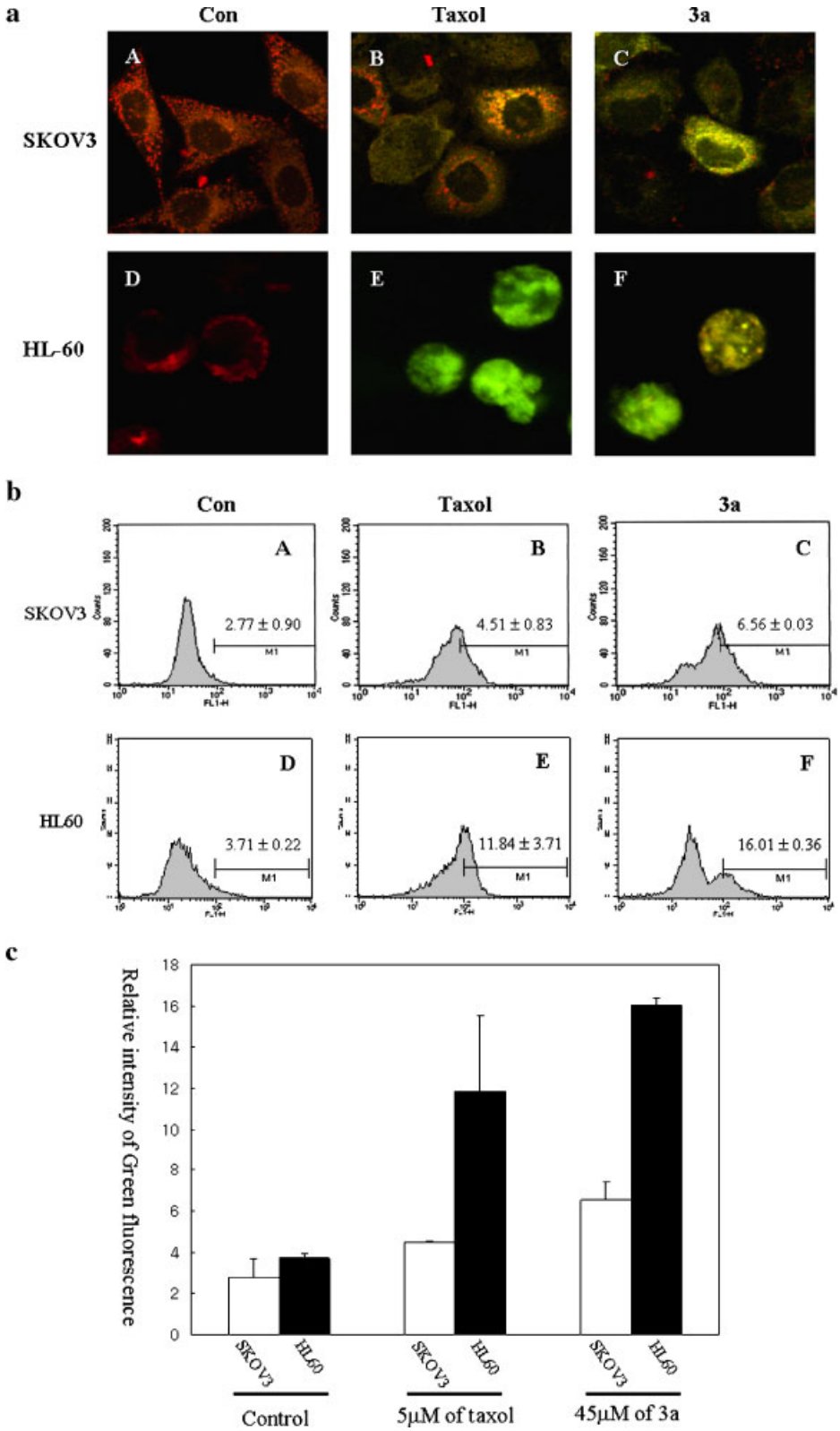
a
Con
Taxol
3a
SKOV3
HL-60
A
B
C
D
E
F
b
Con
Taxol
3a
SKOV3
HL60
2.77 ± 0.90
4.51 ± 0.83
6.56 ± 0.03
3.71 ± 0.22
11.84 ± 3.71
16.01 ± 0.36
M1
FL1-H
c
Relative intensity of Green fluorescence
SKOV3
HL60
Control
5μM of taxol
45μM of 3a

Fig. 3.

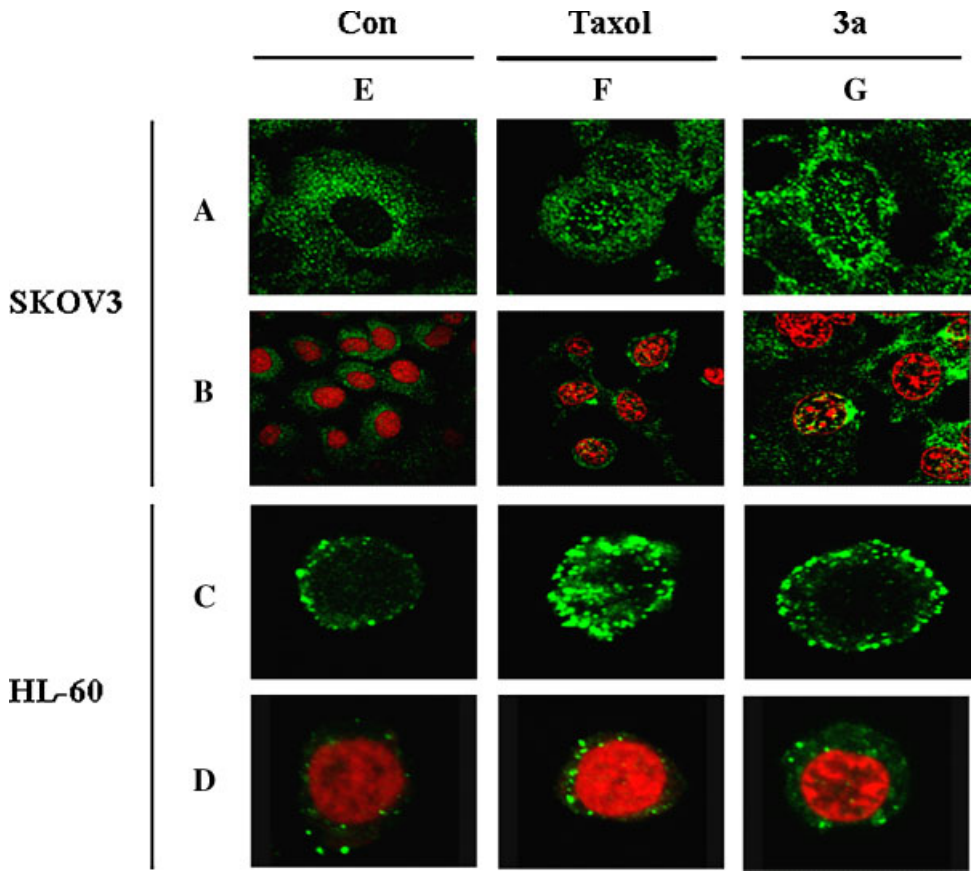

Fig. 4. Localization of AIF (apoptosis inducing factor) following treatment with taxol or **3a**. **A**, **B**: SKOV3 cells; **C**, **D**, HL-60 cells. A and C, stained with an anti-AIF monoclonal antibody (mAb); B and C, stained with an anti-AIF mAb and PI. **E**, untreated cells; **F**, treated with 5 μM taxol; **G**, treated with 45 μM **3a**. In treated SKOV3 cells, AIF is seen in both the cytosol and nucleus, whereas no nuclear translocation is seen in HL-60 cells.

effects, the most likely seems to hinge on the ability of selenium to inhibit cell proliferation [Ip et al., 2000].

Some reports showed that apoptotic signaling involves the activation of the caspase proteases that cleave key protein substrates; numerous reports have shown that caspase inhibition blocks the acquisition of apoptotic traits and prevents mammalian cell death [Joza et al., 2001]. The most commonly activated caspase, caspase-3, cleaves and inactivates the inhibitor of caspase-activated DNase (ICAD), leading to stimulation of CAD, an important DNA fragmentation factor. In vitro and in vivo studies on the interrelationship of caspase-3 and -9 signaling have suggested the existence of four different apoptotic pathways [Hakem et al., 1998; Srinivasula et al., 1998; Cain et al., 1999; Saleh et al., 1999]. As several apoptotic pathways appear to co-exist in mammalian cells, it is important to explore the mechanism of apoptosis induced by drugs that are considered candidates for development as anti-cancer agents.

The results of our study demonstrate that both **3a** and the positive control, taxol, triggered

Fig. 3. Staining with JC-1 in SKOV3 and HL60 cells for assess mitochondrial membrane potential. **a**: **A** and **D**, untreated cells; **B** and **E**, cells treated with 5 μM taxol; **C** and **F**, cells treated with 45 μM **3a.** The results revealed decreased MMP following taxol and **3a** treatment. They were figured by confocal microscopy. **b**: **A** and **D**, untreated cells; **B** and **E**, cells treated with 5 μM taxol; **C** and **F**, cells treated with 45 μM **3a.** The results revealed decreased MMP following taxol and **3a** treatment by flow cytometer. **c**: Open-bar is on SKOV3 cells and closed-bar is HL60 cells. The absorbance at 530 nm increased from 2.77 ± 0.90 (mean $\pm$ SD) in untreated cells to 4.51 ± 0.83 ($P < 0.05$) in taxol-treated cells and 6.56 ± 0.03 in selenium-treated cells ($P < 0.05$) of SKOV3 cells and 3.71 ± 0.22 in untreated cells to 11.84 ± 3.71 ($P < 0.05$) in taxol-treated cells and 16.01 ± 0.36 in selenium-treated cells ($P < 0.05$) of HL60 cells within 24 h. It indicates the relative intensity of maximum green fluorescent emission.

caspase-3-independent apoptosis in a human ovarian cancer cell line. This is consistent with previous reports by our group and others [Ofir et al., 2002; Ahn et al., 2004] that SKOV3 cells showed caspase-3 and caspase-9-independent apoptosis in response to taxol. In contrast, both taxol and **3a** induced caspase-3-associated apoptosis in the HL-60 human acute myelocytic leukemia cell line. Our findings in HL-60 cells were consistent with the previous report in taxol [Ibrado et al., 1998], indicating that taxol may trigger different apoptotic pathways in different cell types.

Recent studies and our previously report have indicated that mitochondria act as the key coordinators of cell death. Several pro-apoptotic signaling pathways converge to induce MMP, often via the Bcl-2 family proteins [Fadeel et al., 1999a, 1999b; Gogvadze et al., 2001]. The outer mitochondrial membrane (OMM) becomes completely permeabilized to proteins, while the inner mitochondrial membrane (IMM) remains intact. This results in leakage of proteins from the mitochondrial intermembrane space [Ravagnan et al., 2002]. Of these, the apoptosis-inducing factor (AIF) is an important released protein that can be translocated to the nucleus in response to death stimuli [Susin et al., 1999; Daugas et al., 2000]. Emerging evidence suggests that translocation of mitochondrial AIF into the nucleus is a hallmark of caspase-independent apoptosis [Cande et al., 2002]. Our data showed that **3a** treatment of SKOV3 cells led to decreases in the MMP and triggered translocation of AIF into the nucleus. Furthermore, flow cytometry revealed that **3a**-treated SKOV3 cells showed DNA fragmentation and accumulation the sub-G1 fraction.

In sum, we herein demonstrated that **3a** effectively inhibits the proliferation of a human ovarian cancer cell line and an acute myelocytic leukemia cell line. Furthermore, we showed for the first time that **3a** triggers a caspase-3-independent pathway involving nuclear translocation of AIF in SKOV3 cells, but did not in HL-60 cells, although mitochondrial membrane depolarization was observed following **3a** treatment of both SKOV3 and HL-60 cells, our results indicate that the downstream apoptotic mechanisms differ in these cell types.

REFERENCES

Ahn HJ, Kim YS, Kim JU, Han SM, Shin JW, Yang HO. 2004. Mechanism of taxol-induced apoptosis in human SKOV3 ovarian carcinoma cells. J Cell Biochem 91: 1043–1052.

Cain K, Brown DG, Langlais C, Cohen GM. 1999. Caspase activation involves the formation of the aposome, a large (approximately 700 kDa) caspase-activating complex. J Biol Chem 274:22686–22692.

Cande C, Cecconi F, Dessen P, Kroemer G. 2002. Apoptosis-inducing factor (AIF): Key to the conserved caspase-independent pathways of cell death? J Cell Sci 115:4727–4734.

Cho DY, Jung U, Chung AS. 1999. Induction of apoptosis by selenite and selenodiglutathione in HL-60 cells: Correlation with cytotoxicity. Biochem Mol Biol Int 47: 781–793.

Clark LC, Cantor KP, Allaway WH. 1991. Selenium in forage crops and cancer mortality in U.S. counties. Arch Environ Health 46:37–42.

Cossarizza A, Baccarani-Contri M, Kalashnikova G, Franceschi C. 1993. A new method for the cytofluorimetric analysis of mitochondrial membrane potential using the J-aggregate forming lipophilic cation 5,5′,6,6′-tetrachloro-1,1′,3,3′-tetraethylbenzimidazolcarbocyanine iodide (JC-1). Biochem Biophys Res Commun 197:40–45.

Daugas E, Susin SA, Zamzami N, Ferri KF, Irinopoulou T, Larochette N, Prevost MC, Leber B, Andrews D, Penninger J, Kroemer G. 2000. Mitochondrio-nuclear translocation of AIF in apoptosis and necrosis. FASEB J 14:729–739.

Ekert PG, Silke J, Vaux DL. 1999. Inhibition of apoptosis and clonogenic survival of cells expressing crmA variants: Optimal caspase substrates are not necessarily optimal inhibitors. EMBO J 18:330–338.

Fadeel B, Orrenius S, Zhivotovsky B. 1999a. Apoptosis in human disease: A new skin for the old ceremony? Biochem Biophys Res Commun 266:699–717.

Fadeel B, Zhivotovsky B, Orrenius S. 1999b. All along the watchtower: On the regulation of apoptosis regulators. FASEB J 13:1647–1657.

Flohe L, Andreesen JR, Brigelius-Flohe R, Maiorino M, Ursini F. 2000. Selenium, the element of the moon, in life on earth. IUBMB Life 49:411–420.

Ganther HE. 1999. Selenium metabolism, selenoproteins and mechanisms of cancer prevention: Complexities with thioredoxin reductase. Carcinogenesis 20:1657–1666.

Gogvadze V, Robertson JD, Zhivotovsky B, Orrenius S. 2001. Cytochrome c release occurs via $Ca2^{+}$-dependent and $Ca2^{+}$-independent mechanisms that are regulated by Bax. J Biol Chem 276:19066–19071.

Hakem R, Hakem A, Duncan GS, Henderson JT, Woo M, Soengas MS, Elia A, de la Pompa JL, Kagi D, Khoo W, Potter J, Yoshida R, Kaufman SA, Lowe SW, Penninger JM, Mak TW. 1998. Differential requirement for caspase 9 in apoptotic pathways in vivo. Cell 94:339–352.

Ibrado AM, Kim CN, Bhalla K. 1998. Temporal relationship of CDK1 activation and mitotic arrest to cytosolic accumulation of cytochrome C and caspase-3 activity during Taxol-induced apoptosis of human AML HL-60 cells. Leukemia 12:1930–1936.

Ip C. 1985. Selenium inhibition of chemical carcinogenesis. Fed Proc 44:2573–2578.

Ip C, Thompson HJ, Ganther HE. 2000. Selenium modulation of cell proliferation and cell cycle biomarkers in normal and premalignant cells of the rat mammary gland. Cancer Epidemiol Biomarkers Prev 9:49–54.

Joza N, Susin SA, Daugas E, Stanford WL, Cho SK, Li CY, Sasaki T, Elia AJ, Cheng HY, Ravagnan L, Ferri KF, Zamzami N, Wakeham A, Hakem R, Yoshida H, Kong YY, Mak TW, Zuniga-Pflucker JC, Kroemer G, Penninger JM. 2001. Essential role of the mitochondrial apoptosis-inducing factor in programmed cell death. Nature 410:549–554.

Koketsu M, Yang HO, Kim YM, Ichihashi M, Ishihara H. 2001. Preparation of 1,4-oxaselenin from AgNO(3)/LDA-assisted reaction of 3-selena-4-pentyn-1-one as potential anti-tumor agents. Org Lett 3:1705–1707.

Lu J, Kaeck M, Jiang C, Wilson AC, Thompson HJ. 1994. Selenite induction of DNA strand breaks and apoptosis in mouse leukemic L1210 cells. Biochem Pharmacol 47: 1531–1535.

Lu J, Jiang C, Kaeck M, Ganther H, Vadhanavikit S, Ip C, Thompson H. 1995. Dissociation of the genotoxic and growth inhibitory effects of selenium. Biochem Pharmacol 50:213–219.

Ofir R, Seidman R, Rabinski T, Krup M, Yavelsky V, Weinstein Y, Wolfson M. 2002. Taxol-induced apoptosis in human SKOV3 ovarian and MCF7 breast carcinoma cells is caspase-3 and caspase-9 independent. Cell Death Differ 9:636–642.

Ormerod MG, Collins MK, Rodriguez-Tarduchy G, Robertson D. 1992. Apoptosis in interleukin-3-dependent haemopoietic cells. Quantification by two flow cytometric methods. J Immunol Methods 153:57–65.

Ravagnan L, Roumier T, Kroemer G. 2002. Mitochondria, the killer organelles and their weapons. J Cell Physiol 192:131–137.

Saleh A, Srinivasula SM, Acharya S, Fishel R, Alnemri ES. 1999. Cytochrome c and dATP-mediated oligomerization of Apaf-1 is a prerequisite for procaspase-9 activation. J Biol Chem 274:17941–17945.

Schrauzer GN. 2000. Anticarcinogenic effects of selenium. Cell Mol Life Sci 57:1864–1873.

Shen HM, Yang CF, Ong CN. 1999. Sodium selenite-induced oxidative stress and apoptosis in human hepatoma HepG2 cells. Int J Cancer 81:820–828.

Srinivasula SM, Ahmad M, Fernandes-Alnemri T, Alnemri ES. 1998. Autoactivation of procaspase-9 by Apaf-1-mediated oligomerization. Mol Cell 1:949–957.

Susin SA, Lorenzo HK, Zamzami N, Marzo I, Snow BE, Brothers GM, Mangion J, Jacotot E, Costantini P, Loeffler M, Larochette N, Goodlett DR, Aebersold R, Siderovski DP, Penninger JM, Kroemer G. 1999. Molecular characterization of mitochondrial apoptosis-inducing factor. Nature 397:441–446.

Van Engeland M, Ramaekers FC, Schutte B, Reutelingsperger CP. 1996. A novel assay to measure loss of plasma membrane asymmetry during apoptosis of adherent cells in culture. Cytometry 24:131–139.

Zamzami N, Kroemer G. 1999. Condensed matter in cell death. Nature 401:127–128.